

## Mechanical properties of biological specimens explored by atomic force microscopy

This article has been downloaded from IOPscience. Please scroll down to see the full text article.

2013 J. Phys. D: Appl. Phys. 46 133001

(<http://iopscience.iop.org/0022-3727/46/13/133001>)

View [the table of contents for this issue](#), or go to the [journal homepage](#) for more

Download details:

IP Address: 128.178.66.186

The article was downloaded on 19/06/2013 at 13:34

Please note that [terms and conditions apply](#).

## TOPICAL REVIEW

# Mechanical properties of biological specimens explored by atomic force microscopy

S Kasas<sup>1,2</sup>, G Longo<sup>1</sup> and G Dietler<sup>1</sup><sup>1</sup> Laboratoire de Physique de la Matière Vivante, EPFL, CH-1015 Lausanne, Switzerland<sup>2</sup> Département de Neurosciences Fondamentales, Université de Lausanne, CH-1005 Lausanne, SwitzerlandE-mail: [sandor.kasas@epfl.ch](mailto:sandor.kasas@epfl.ch)

Received 4 December 2012, in final form 16 January 2013

Published 26 February 2013

Online at [stacks.iop.org/JPhysD/46/133001](http://stacks.iop.org/JPhysD/46/133001)**Abstract**

The atomic force microscope is a widely used surface scanning apparatus capable of reconstructing at a nanometric scale resolution the 3D morphology of biological samples. Due to its unique sensitivity, it is now increasingly used as a force sensor, to characterize the mechanical properties of specimens with a similar lateral resolution. This unique capability has produced, in the last years, a vast increase in the number of groups that have exploited the versatility and sensitivity of the instrument to explore the nanomechanics of various samples in the fields of biology, microbiology and medicine. In this review we outline the state of the art in this field, reporting the most interesting recent works involving the exploration of the nanomechanical properties of various biological samples.

(Some figures may appear in colour only in the online journal)

**1. Introduction**

Atomic force microscopy (AFM) [1] is a surface scanning technique initially developed to image non-conductive samples at a high resolution. Unlike its predecessor, the scanning tunnelling microscope [2], the AFM allows performing measurements under any environmental conditions, including in liquid or in physiological media. This has opened the use of this technique to the field of biology, delivering a means to perform high-resolution imaging of specimens in their natural state, as are, for instance, living cells.

Soon after its invention, it appeared clear that the AFM could be used to investigate other surface characteristics of specimens. For instance, by collecting the lateral deflections of the cantilever, the surface's local tribological properties were determined. On the other hand, the study of the vertical deformations of the cantilever when interacting with the surface can provide valuable information on the mechanical properties of the sample. Since 1990, starting from single

proteins up to whole tissues or organs, virtually every category of living organism had its stiffness and Young's moduli explored by AFM. These studies indicate how mechanical properties play a significant role in defining the characteristics and functionality of biological and living systems and that several pathological conditions are associated with stiffness or adhesion modifications. This opens new ways in the characterization of biological systems from single molecular assemblies up to whole tissues and proposes the use of AFM as a diagnostic tool for the study of the mechanical properties of these specimens.

The present review is mainly focused on the use of AFM techniques to characterize the stiffness of biological samples. This choice is motivated by the wide distribution of the instrument in biologically oriented laboratories and its ease of use for such an investigation. We will focus on the most recent results obtained on living organisms ranging from viruses and bacteria to fungi, to eukaryotic plant and animal cells. Readers interested in the mechanical properties of smaller structures,

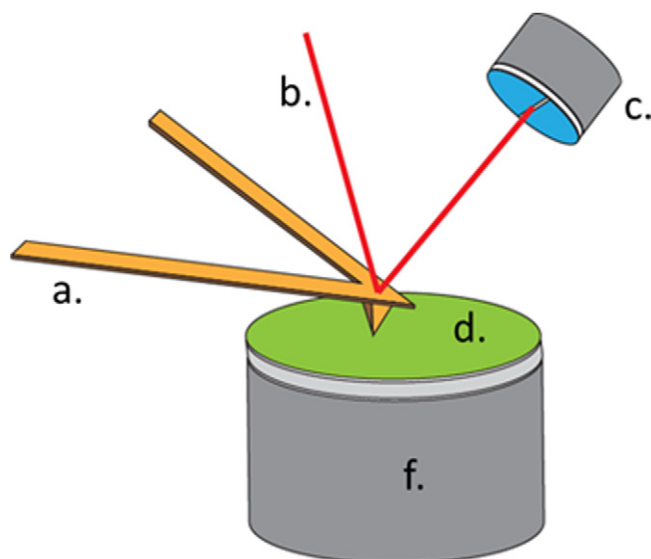


**Figure 1.** Schematics of an AFM. (a) cantilever and tip, (b) laser beam, (c) two or four segment photodiode, (d) sample, (f) piezo actuator.

i.e. single molecules and protein assemblies, are invited to refer to the excellent review of Kurland *et al* [3].

## 2. Brief description of an atomic force microscope

As previously described, the main component of an AFM (figure 1) is a cantilever that has, at its end, a microfabricated tip. This is the actual sensing device and its dimensions and geometry considerably influence the achievable resolution. Typically, tips are pyramidal and have an apical radius between 10 and 50 nm (smaller tips with apical radius of  $\sim 1$  nm can be obtained for particular applications). AFM cantilevers are usually made of silicon or silicon nitride and have two shapes: rectangular and ‘V’-shaped. Their length varies between 200 and  $2\ \mu\text{m}$  and with a spring constant in the range  $0.01$ – $100\ \text{N m}^{-1}$ . The face of the cantilever that is not in contact with the sample is usually coated with a metallic thin layer (often chromium/gold) in order to enhance reflectivity.

A piezoactuator is used to raster-scan the tip over the sample and to maintain it at a very small distance from the surface of the sample. This piezoactuator can perform minimal displacements of the order of  $1\ \text{\AA}$  with high precision and can scan areas in the order of  $100\ \mu\text{m}$ .

During this scan, the tip–sample interactions induce deformations of the cantilever. A controller regulates, collects and processes the data, and drives the piezo scanner in order to reconstruct a 3D topography of the scanned area.

The cantilever deflections may be measured in different ways in order to reproduce the sample topography. The most common technique is the optical lever method: a laser beam is focused on the coated back side of the cantilever and the reflected beam is detected by means of a position sensor, which is usually a quartered photodiode. In this configuration both cantilever vertical and lateral (torsion) deflections may be collected.

An AFM measurement can be performed in mainly two modalities: contact and non-contact. In the contact modality the tip is brought in mechanical contact with the sample surface. In this region the predominant forces are strongly repulsive interactions that typically deflect the cantilever. This modality is also known as constant force and the imaging of the surface is obtained by maintaining a fixed cantilever deflection while scanning. The forces that are typical of this modality are related directly to the cantilever spring constant and the chosen working deflection, and are usually in the order of  $1$ – $10\ \text{nN}$ .

Since the forces involved in the contact modality may be very high especially when soft samples are concerned, a dynamic mode was introduced in 1993 by Zhong *et al* [4]. In this configuration, the tip is placed in oscillation close to its resonance frequency (base frequency) over the sample’s surface. When the tip begins to interact with the sample (or to briefly touch the surface—tapping mode) these surface forces modify the oscillation amplitude of the cantilever and this is commonly used as feedback to control the tip–sample distance and to record the topography of the specimen. This exploits the high resolution typical of the contact modality while applying a very low force to the sample, thus minimizing the sample deformation and damage.

The basic principle of the AFM to measure forces or to measure interactions between a sharp tip and the sample surface led to the creation of a variety of other scanning probe microscopes (SPMs), such as the magnetic force microscope (MFM), the dynamic force microscope (DFM), the friction force microscope (FFM), and the electrostatic force microscope (EFM). This provides the unique opportunity to characterize a single nm-sized spot by a combination of methods and therefore gain more information than by the separate application of a single method.

## 3. Measurement of mechanical properties by AFM

A cantilever is a very reliable and sensitive force-sensor and this makes the AFM an ideal tool to probe, through this sensor, the mechanical properties of specimens with unparalleled resolution and sensitivity [5].

Such characterizations can be carried out by performing a force, or force–distance curve (figure 2): the tip is lowered towards the sample and pressed against it while the deflection of the cantilever is recorded (approach-curve); next, the tip is retracted from the sample and back to its starting position (withdrawal curve) (in several configurations, the sample is moved towards and away from the tip. Naturally this changes nothing in the description of the process).

By analysing an approach force curve, the mechanical properties (i.e. stiffness, Young’s modulus) of the soft sample can be obtained. On the other hand, the area between the negative part of the withdrawal curve and the Z-axis can provide insight into the adhesion properties and, if the tip is adequately functionalized, can be used to study specific molecule–molecule interactions.

The first study on force–distance curves acquired with an AFM, concerned the characterization of surface forces on LiF and graphite [6].

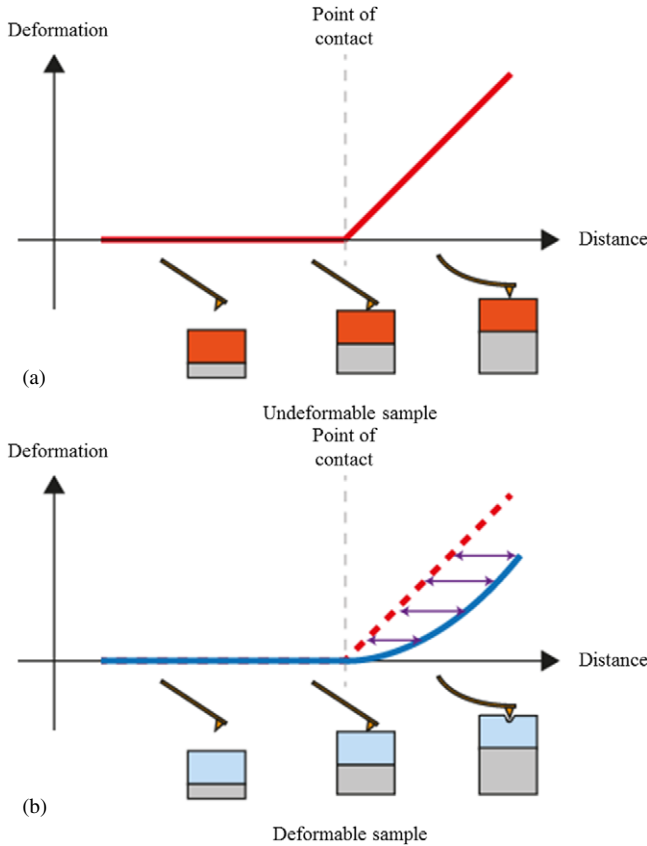


**Figure 2.** Force–distance curves recorded on a hard (a) and a soft sample (b). An indentation curve can be obtained by subtracting one curve from the other (violet arrows).

In 1991 several studies of force–distance curves in liquids were performed, theoretically and experimentally, actively opening the way to the characterization of soft, biological specimens.

The first works trying to interpret force–distance curves and related information appeared in 1989–1990. Since the cantilever is generally considered as a perfect Hookian spring, the applied force can be defined as

$$F = k \cdot dx$$

where  $F$  is the force applied,  $k$  is the spring constant of the cantilever and  $dx$  is the amplitude of cantilever bending.

The force curve depicts the vertical deformation of the cantilever (i.e. the applied force) versus the vertical position of the sample. A particularly important feature in this curve is the point of contact: when, during its approach towards the sample, the tip comes in contact with the surface.

If the sample is undeformable (i.e. much harder than the cantilever), after coming in contact with its surface, the tip will not continue its descent and the bending of the cantilever will be equal to its vertical displacement. However, if the sample is soft, during its approach the tip will indent (i.e. penetrate) it and the bending of the cantilever will be lower than its vertical displacement. Both cases are illustrated in figure 2.

First of all a force curve collected on an undeformable substrate must be subtracted from the soft sample curve. This

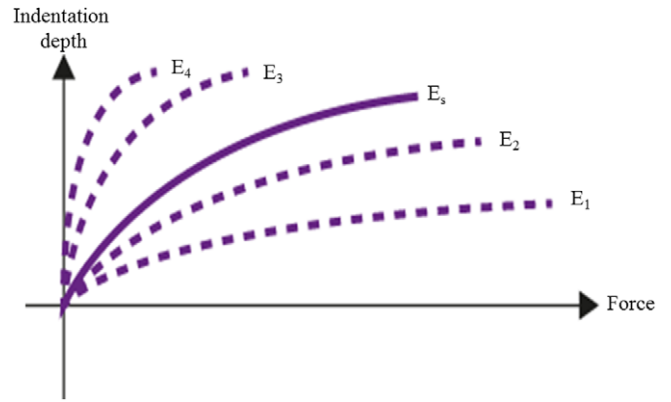


**Figure 3.** A numerical value ( $E_s$ ) can be obtained by fitting the experimental indentation curve (plain line) with theoretical models such as those of Hertz or Sneddon (dashed lines).

indentation curve indicates the force needed to apply to the tip to indent it (i.e. to push it) into a defined depth of the sample. The numerical value of Young’s modulus is obtained by fitting this indentation curve with one of several available theoretical models such as those of Hertz [7], Sneddon [8], JKR [9] or Tataru [10] as depicted in figure 3.

The Hertz model describes the elastic deformation of two spheres and states that the force is proportional to the power of 1.5 of the deformation. However, it does not consider electrostatic forces, adhesion or friction (i.e. lateral, tangential forces) between contact surfaces.

Sneddon’s model extends the calculation to other geometries but still does not account for long range forces. Usually the AFM tips have a four-sided pyramidal shape and their very end can be modelled by a cone or a paraboloid. In this case the indentation depth  $\delta$  and the applied force  $F(\delta)$  are connected through

$$F(\delta) = \frac{2 \tan(\alpha)}{\pi} E' \delta^2 \quad \text{for conical tips}$$

and through

$$F(\delta) = \frac{4\sqrt{R}}{3} E' \delta^{1.5} \quad \text{for paraboloidal tips,}$$

where  $\alpha$  is the opening angle and  $R$  is the radius of curvature of the tip. Since these formulae include the contribution from the tip and from the sample,  $E'$  corresponds to what is referred to as the reduced Young’s modulus.

If  $E_{\text{sample}} \ll E_{\text{tip}}$ , then the sample’s Young’s modulus  $E_{\text{sample}}$  can be related to the reduced Young’s modulus  $E'$  through

$$\frac{1}{E'} = \frac{1 - \mu_{\text{sample}}^2}{E_{\text{sample}}},$$

where  $\mu$  is the Poisson ratio of the sample (ranging 0 to 0.5) that reflects the compressibility of the sample and its maximal value corresponds to an incompressible material. A value of 0.5 is usually assumed for cells.

The JKR model takes account of adhesive forces, whereas the Tataru model simulates a sphere sandwiched between two parallel plates. This last model is essentially used to interpret

AFM data recorded on small samples such as single proteins. For practical reasons the most widely used models are those of Hertz and Sneddon. A detailed description of the different available models can be found in Cappella and Dietler [11] and Butt *et al* [12].

It should be mentioned that these models are relatively limited since they consider the AFM tip as well the sample to be homogeneous and having a well-defined geometry. These are conditions that rarely reflect the experimental situation encountered during AFM measurements on biological samples. More precise models can be obtained by numerical simulations using the finite element method [13]. In this case a virtual tip is simulated to indent a virtual sample of arbitrary shape possessing arbitrary mechanical properties. The simulation results in a virtual force–distance curve. During several simulation runs, the geometry and/or the characteristics of the sample are modified to match the experimental force–distance curve.

To construct a stiffness map of the sample, several force–distance curves are recorded successively all over the surface to form a force–volume map. Such a data set is typically composed of  $32^2$  or  $64^2$  pixels, i.e. force–distance curves that are eventually processed in parallel to obtain topography, stiffness or adhesion maps of the sample. In this modality the tip is moved, as a function of time, using a typical triangular or trapezoidal waveform. The major drawback of this imaging mode is its limited spatial and temporal resolution. Recording a single file can require long acquisition times (up to 1 h), depending on the speed of the single force curve and on the number of pixels.

Recently, alternative solutions have been developed by several AFM manufacturers such as the QI™ (Quantitative Imaging) mode of JPK Instruments or the peak force tapping of Bruker. These modes basically consist in oscillating the cantilever in the vertical direction with limited amplitude and a high frequency (0.25–2 kHz). The cantilever is driven in a continuous movement using a sinusoidal or sinusoid-like waveform rather than a triangular one and the resulting force–distance curves are recorded. The data set is almost equivalent to a classical force–volume file with a considerable gain in terms of recording speed and resolution ( $512^2$  pixels images).

A relatively recent approach, called the rate-jump method [14, 15], has been developed to measure with high precision the stiffness of soft biological samples. The approach is inspired from the indentometry techniques that are in use in material sciences and that have been developed to dissociate the viscous from the elastic components that both influence the classical indentation measurements. As an illustration, indenting a viscoelastic sample at a low speed will make it appear softer than in measurements at higher speeds. The difference between the two measurements is due to the viscous properties of the sample. A rate-jump measurement consists in indenting the sample at a given speed up to a certain depth, typically  $1\ \mu\text{m}$ . At this point, the indentation process is interrupted and the tip is maintained at rest for a couple of seconds. Finally, the tip is retracted also at a given speed. The deformation of the cantilever during the retraction cycle is used to calculate the sample's Young's modulus. The main

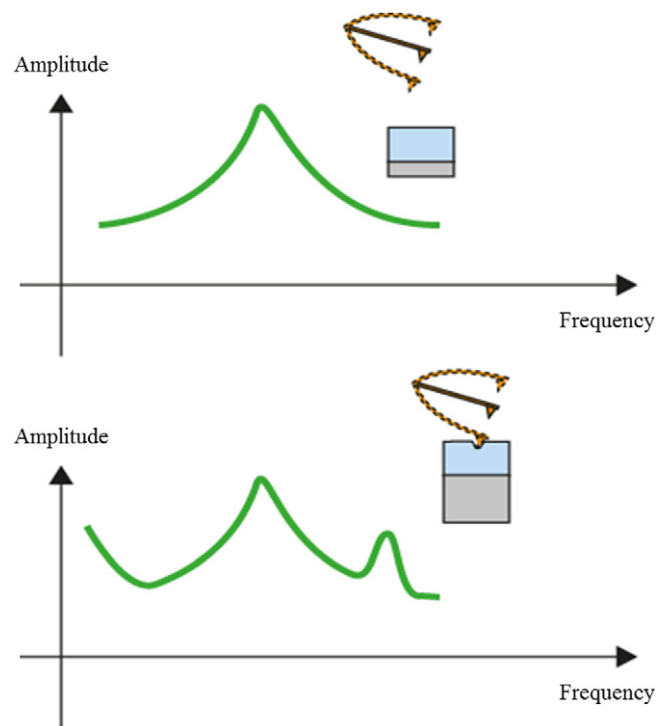


**Figure 4.** Illustration of the dynamic mode: novel resonances appear when the oscillating tip approaches the surface of the sample (the amplitude of the higher frequency harmonic is exaggerated for illustrative purposes)

advantage of the method resides in the absence of viscous contribution of the sample in the collected data. However, this increase in precision is obtained at the price of a dramatic loss of temporal and spatial resolution. A single indentation cycle on living cells lasts up to 40 s and since the tip is usually a cylinder with a diameter of  $1\ \mu\text{m}$  the spatial resolution is also strongly reduced. This technique was successfully applied on various living cancer cells [15].

Another set-up that is employed to perform fast mechanical investigations of soft samples was introduced by Martin *et al* in 1987 [16] and stems directly from the dynamic acquisition mode of the AFM: the tip is placed in oscillation close to its resonance frequency over the sample's surface. When the oscillation of the tip brings it to briefly touch the surface (tapping mode) the interaction between the tip and the sample modifies both the amplitude and the phase of the oscillations of the cantilever (phase lag) and this change is related to the energy lost per oscillation cycle due to the interaction. Since this is dependent on the stiffness of the sample, the phase variations can deliver information regarding its surface properties [17].

A more precise determination can be obtained by considering that the tip–sample interaction is non-linear, and modifies the tip oscillation producing new resonances that are harmonics of the base frequency.

These contain as well information on the stiffness of the sample and can be detected using additional lock-in amplifiers (see figure 4).

Since the dynamic AFM imaging mode is extremely fast (one or two orders of magnitude higher than the conventional

force-volume mode), it can be expected that this modality will provide a new and fruitful means to map at high spatial and temporal resolution the mechanical and adhesion properties of samples [18]. The main drawbacks of the dynamical mode reside in the relative complexity of set-up and in the difficulty to correlate the obtained signal with a specific Young's modulus value.

All these modalities allow the determination of the surface properties of specimen. Several novel techniques are arising to obtain information of the properties of the inner content of samples.

One of these systems, called the scanning near-field ultrasonic holography, consists in oscillating the sample at megahertz frequencies while an AFM cantilever is placed in contact with the sample's surface. The ultrasonic waves that are travelling through the sample also drive the cantilever.

If the cantilever is in addition vibrated at a slightly different frequency, the non-linear coupling between the two oscillators may be used to gather information on the sample's elastic properties as well its inner structures [19, 20].

An alternative is to process force–distance or indentation curves in order to obtain information regarding the properties of the material present underneath the surface of the samples. As described before, Young's modulus is obtained by fitting an indentation curve with theoretical models such as those of Hertz or Sneddon. However, such a processing has the drawback to sum the mechanical contribution of all the structures encountered by the tip along its indentation path. By dividing the indentation curve in small segments and by applying the Hertz or Sneddon model on each of them, stiffness differences present along the indentation path can be highlighted. This 'simple' additional processing step permits distinguishing structures located underneath the sample's surface with a contrast that reflects their stiffness [21]. Figure 5 depicts the procedure used to reconstruct a stiffness tomogram.

#### 4. Viruses

Viruses are, after prions, the smallest known infectious organisms and, depending on the definition of life, the smallest living organisms. Their size varies between 20 and 300 nm and they consist of genetic material made from DNA or RNA, a protein coat or capsid and, in some cases, an envelope of lipids that surrounds the protein coat. Viral capsids are generally formed by several copies of a limited amount of different proteins. They are symmetrical closed structures whose mechanical properties are essential for setting optimal functionality. The study of viruses is not limited to fundamental research and virology but also for pharmacology, since they can be used as nanocontainers for drug delivery [22]. The first reports on AFM imaging of viruses appeared in 1992 [23, 24]. However, these studies were more motivated by the search for reliable calibration tools rather than fundamental virological questions. The first report of the determination using AFM of Young's moduli of viruses can be found in Vesenska *et al* in 1993 [25]. In this study the authors tested the compressibility of tobacco mosaic virus (TMV) by tips of

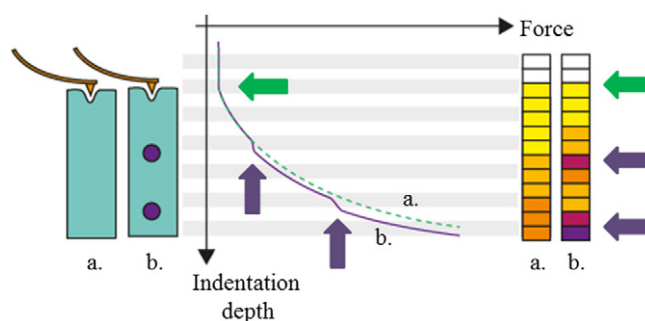


**Figure 5.** Stiffness tomography: comparison between the indentation of a soft homogeneous sample (a) and one containing two hard inclusions, located at different depths (b). Left subfigure: the two soft samples indented by the AFM tip. Sample (a) is homogeneous, whereas sample (b) contains two hard inclusions symbolized by two violet circles. Middle subfigure: the corresponding (rotated) force–distance curves recorded on samples (a) (green dashed line) and (b) (violet continuous line). The violet arrows indicate where the force–distance curve recorded on the (b) sample presents kinks that appear when the AFM tip starts to 'feel' the hard inclusions. The green arrow represents the point of contact. Right subfigure: the reconstructed stiffness profile of the two samples. The violet arrows indicate the estimated positions of the hard inclusions.

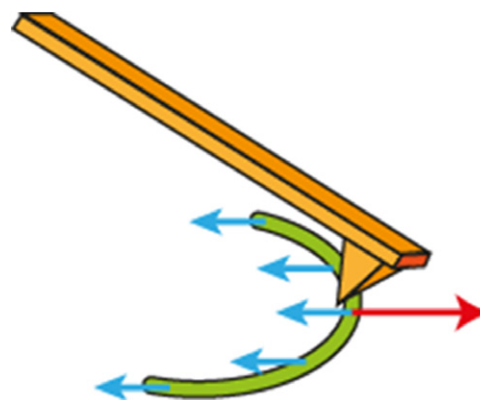


**Figure 6.** Illustration of the use of lateral friction between the mica surface (not shown) and TMV (depicted as a green tube) to estimate Young's modulus of the virus.

various radii. They found that a measurable deformation of the virus occurs at a pressure in the range of 1 MPa whereas irreversible damage is induced above 40 MPa. In 1997 Falvo *et al* [26] used lateral friction between the TMV and mica to estimate its Young's modulus and deformability.

In these experiments the authors used an AFM tip to apply a force in the direction normal to the contact area between the TMV and the substrate surface (red arrow in figure 6).

By modelling this experimental set-up by a beam bending under a uniformly distributed load (blue arrows) the authors found Young's modulus value of 1 GPa for TMV. It should be mentioned that these experiments were carried out in air.

The first indentation experiments on viruses in liquid medium were reported in 2004 [27] on empty capsids of  $\Phi 29$ . This is a widely used microorganism (bacteriophage, i.e. a virus that infects bacteria) to study basic biochemical reactions such as DNA replication and transcription. These experiments

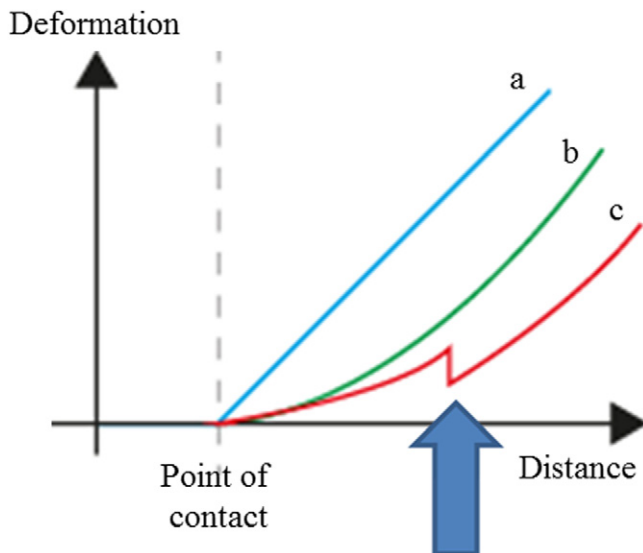


**Figure 7.** Force–distance curves recorded on mica (a), unbreakable soft sample (b) and empty virus capsids (c). The breaking of the virus capsid produces a discontinuity in the force–distance curve, pointed out by the blue arrow.

revealed that the capsid's Young's modulus was about 1.8 GPa. The authors also found that the empty capsid breaks beyond indentations of 12 nm and an applied force of 2.8 nN. The breakage of the capsid is testified by a sudden jump in the force–distance curve as depicted in figure 7.

Numerous other indentation experiments explored the influence of the presence of the genetic material on the mechanical properties of viral capsids. Experiments were carried on empty and full capsids of various viruses such as CCMV (cowpea chlorotic mottle virus, a virus that infects cowpea plants) [28], MVM (parvovirus minute virus of mice, which is among the smallest and structurally simplest viruses known) [29] or HSV1 (human herpes simplex virus type 1, a highly contagious virus that widely infects humans) [30, 31].

Interestingly this latter study revealed that empty and DNA-containing HSV1 capsids shared the same mechanical properties.

Another set of very interesting experiments explored the changes of Young's moduli of viruses during their maturation. Certain types of viruses such as retroviruses (viruses that store their genetic information in RNA instead of DNA and that translate it in DNA during their duplication in host cells) undergo substantial morphological changes after budding from the host cell. Experiments on MLV (Moloney murine leukemia virus) [32] and HIV (human immunodeficiency virus) [33] both reported softening of their capsid during maturation. This modification seems to promote virus entry into cells. Conversely, an increase in Young's modulus was recently observed in the maturation process of the bacteriophage HK97 as well a rise of the capsid ultimate strength (maximum stress that the capsid can withstand before breaking) [34].

One of the challenges in experiments involving indentation of viruses is the interpretation of the force–distance curves. Since viruses are small structures and possess relatively complex geometries, the classical Hertzian

or Sneddon interpretations do not apply. Therefore, only numerical simulations such as finite element modelling [35] or molecular dynamics (MD) approaches [36] can permit interpretation of experimental results at the molecular level. However, none of these techniques is perfect: MD simulations are computationally expensive and FEM requires *a priori* knowledge of the elastic properties of the capsid. Therefore, recently Roos *et al* [34] employed a mixed technique of MD and normal mode analysis of elastic networks models to simulate indentation of the bacteriophage HK97 and determine their Young's modulus.

Readers interested in the exploration of viruses by AFM can refer to the relatively recent and very complete review paper of Baclayon *et al* [37].

## 5. Bacteria

Bacteria are among the very first forms of life that appeared on Earth. Nowadays their biomass largely exceeds that of all plants and animals. They are present in most habitats on the planet starting from the depth of the Earth's crust up to the human digestive tract. Interestingly there are about ten times more bacteria cells in the human flora than there are human cells [38]. Bacteria measure typically between 0.3 and 5  $\mu\text{m}$  in length and display a wide diversity of shapes such as spheres (cocci), rods (bacilli), spirals (spirilla) or tight coils (spirochaetes). They do not contain a nucleus and are therefore referred to as prokaryotes. Bacteria are broadly classified into Gram- positive and Gram-negative according to their reaction to the Gram stain.

Pioneering studies of the mechanical properties of bacteria were conducted in 1996 by Xu *et al* [39] who investigated the elastic properties of the sheath of the Gram-negative *Methanospirillum hungatei*, bacteria often used to anaerobically treat organic wastes. Remarkably very high Young's modulus values were found (20–40 GPa), suggesting that these microorganisms can withstand an astonishingly high internal pressure of 400 atm. Eventually Amoldi *et al* [40] measured the stiffness (42  $\text{mN m}^{-1}$ ) of the cell wall of a helical, Gram-negative magnetotactic (i.e. having the capacity to orient according to Earth's magnetic field) bacteria (*Magnetospirillum gryphiswaldense*). Later, in 2002, Velegol and Logan [41] explored different strains of *Escherichia coli*, a very common Gram-negative bacterium. The different strains were characterized by the presence of different lipopolysaccharides on their surface and the authors studied their impact on the elasticity and adhesive properties of the bacteria. Abu-Lail and Camesano [42] measured the stiffness of the biopolymeric coating (brush layer) of *Pseudomonas putida* in different potassium chloride concentrations. They demonstrated that the elastic constant as well as the height of the brush layer varies significantly as a function of the ionic strength. Similar experiments were conducted by Gaboriaud *et al* [43] on *Shewanella putrefaciens* by varying the pH of the imaging solution. The authors observed that a rise in pH induces an increase in height and a decrease in the stiffness of the bacterial envelope. In a following study Gaboriaud *et al* [44] observed *Shewanella putrefaciens*, a Gram-negative

bacterium that is responsible for the odour of rotting fish, in force-volume mode. They observed that the bacterium is not a homogeneous structure but that its surface is formed by stiffer and softer domains. In a similar type of study, Francius *et al* [45] observed dramatic differences in the stiffness between the wild type *Lactobacillus rhamnosus* and one of its mutants (CMPG5413). The mutant was found to be two times stiffer than the wild type, presumably due to differences in the surface appendages (the exopolysaccharide layer in this case) between the two strains.

In a nutrient-deprived environment some bacteria such as *Bacillus* or *Clostridium* can undergo a differentiation process (called sporulation) in which the cells synthesize a series of polymer and protein barriers (of a thickness of 100–200 nm) which protect the cell from external stress. The spores are metabolically dormant and constitute one of the most resistant life forms. Once nutrients become available the spores transform (germinate) into their vegetative form and become pathogenic. Recently Pinzón-Arango *et al* [46] measured the stiffness of *B. anthracis* before and after germination. *B. anthracis* causes fatal airborne diseases such as the pulmonary anthrax. The authors measured the spores to be 15 times stiffer than the vegetative forms (200 MPa versus 35 MPa).

When bacteria grow and multiply, they frequently undergo phenotypic modifications in order to embed within a self-produced matrix of extracellular polymeric substance called biofilm. The viscoelastic properties of these films determine their structural integrity, resistance to stress, ease of dispersion and therefore their pathogenicity. Lau *et al* [47] studied the mechanical and adhesive properties of different types of biofilms produced by *Pseudomonas aeruginosa*. It is a Gram-negative bacterium, frequently found on medical equipment such as catheters and that is responsible for numerous nosocomial infections in patients with compromised host defense mechanisms.

As previously mentioned, numerous bacteria have their cell wall decorated by surface appendages (pili, fimbriae, exopolysaccharides or flagella). These structures may protrude several hundreds of nanometres from the cell wall and are involved in numerous bacterial physiological processes such as motility, adhesion, cell–cell interaction or pathogenicity. Francius *et al* [48] studied by AFM the effect of different surface appendages on the mechanical properties of *Escherichia coli* mutants. The study was conducted in different ionic strengths and it revealed that the cell's Young's modulus and turgor pressure depend not only on the ionic strength of the surrounding medium but also on the presence of specific appendages.

Previously, similar studies concerning cell appendages and bacterial stiffness of *Haemophilus influenzae* were conducted by Arce *et al* [49]. This microorganism is a common commensal of the human airways but that can also be responsible for serious infections such as pneumonia or meningitis. The authors found significant differences between the mechanical properties of *H. influenzae* PittGG strains that possess pili and those who do not have these structures.

Whooping cough is a highly infectious disease transmitted by *Bordetella pertussis*, Gram-negative bacteria. Arnal *et al*

[50] used force-volume imaging to map rigid structures present on the bacterial envelope and to detect the presence of various adhesins that are exposed on its surface. As their name suggests, adhesins are molecules that promote the attachment of bacteria to surfaces and therefore play an important role in their virulence. The study suggested a direct correlation between the presence of adhesins and an increase in the average membrane stiffness. Moreover, the stiffness maps revealed an inhomogeneous spatial distribution of Young's modulus of the cell as well the presence of rigid nanodomains on the cell surface.

Similarly stiffness inhomogeneities were observed on the surface of *Escherichia coli* by Longo *et al* [51]. The authors highlighted the dynamical behaviour of these domains and using stiffness tomography imaging could also reveal the presence of stiff structures present underneath the cell surface (see figure 8).

One of the drawbacks of the classical force-volume imaging is its lack of temporal and lateral resolution (as already mentioned in the introduction). Recently Raman *et al* demonstrated how to circumvent these limitations by employing dynamical mode imaging to explore the mechanical properties of *Escherichia coli* [18].

Readers interested in recent review papers concerning the applications of AFM in microbiology that are not limited to the exploration of their mechanical properties can refer to the following publications [52–55], whereas pioneering studies on the stiffness of bacteria are very clearly reviewed in Dufrêne 2001 [56] as well as in [57–59].

## 6. Yeast cells

Yeasts are eukaryotic, usually unicellular microorganisms. Their size varies between 4 and 40  $\mu\text{m}$  and they play important roles in numerous industrial and health domains. The most famous, *Saccharomyces cerevisiae* converts carbohydrates in  $\text{CO}_2$  and alcohols and is nowadays the most thoroughly researched eukaryotic microorganism. Most yeasts reproduce by mitosis and many do so by a specific division process in which the new organism develops as an outgrowth (bud) of another one and separates from its parent organism only when it is mature. Touhami *et al* [60] were among the first to study the mechanical properties of the cell wall of *S. cerevisiae* using AFM. This wall constitutes 25–50% of the volume of the cell and is essentially composed of a microfibrillar array of linked polysaccharides ( $\beta$ -1,3 glucan) overlaid by an outer layer of  $\beta$ -1,6 glucan and mannoprotein [61]. An important minor component of the wall is chitin (polysaccharide of ( $\beta$ -1,4)-linked *N*-acetylglucosamine), which contributes to the insolubility of the fibres in yeast and strengthens the supportive structures of numerous other organisms (such as the exoskeletons of arthropods mollusks and insects). It is believed that chitin plays an important role in stiffening the region of the cell wall involved in budding. By analysing force-volume data recorded on *S. cerevisiae* bud scars, the authors demonstrated that this region was about 10 times stiffer (6 MPa) than the surrounding cell wall (0.6 MPa), which is consistent with an accumulation of chitin in this area.

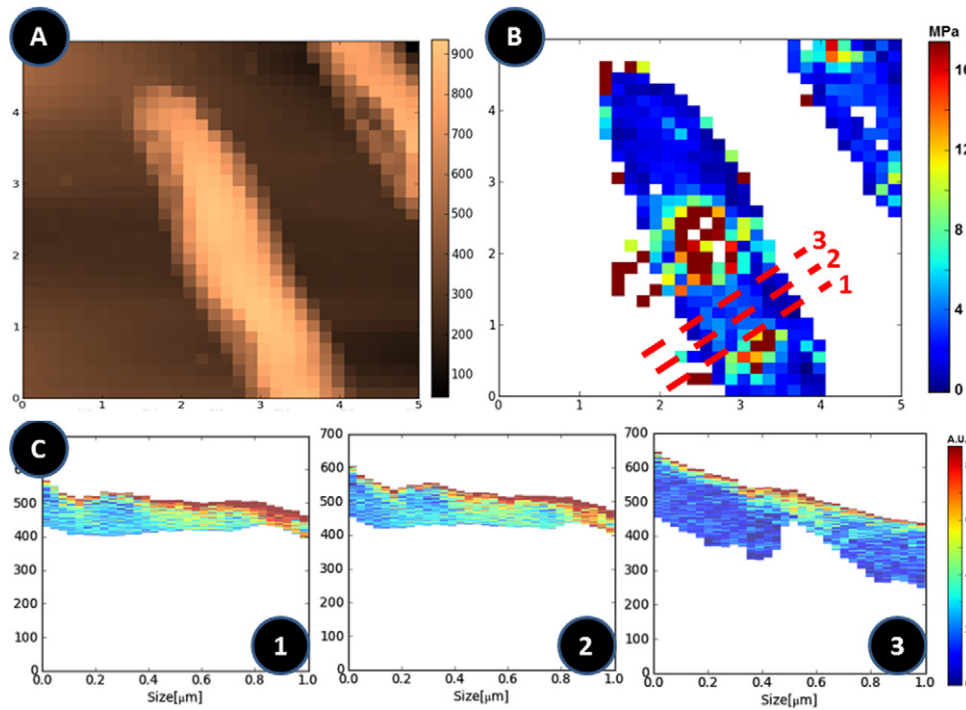


**Figure 8.** Stiffness tomography exploration of bacterial cells. (a) depicts a classical force-volume image of an *E. coli* bacterium. (b) shows the corresponding stiffness map with soft areas coloured in blue and stiffer domains in red. The two stiff areas probably correspond to nucleoids (protein or DNA aggregates in the cytoplasm). (c) The three lower subfigures represent stiffness tomography slices through the bacterial cell, collected in correspondence to the lines in (b), evidencing the presence of stiffer features lying deep under the cell membrane.

A very extensive study of Young's modulus of *S. cerevisiae* was recently conducted by Arfsten *et al* [59]. The study highlighted the influence of the indentation spot and the osmotic pressure on the computed mechanical parameters.

An exploration of the properties of polyelectrolyte encapsulated *S. cerevisiae* was conducted by Svaldo-Lanero in 2007 [62]. This type of study is motivated by the increasing number of applications of encapsulated living organisms in numerous fields of biotechnology and medicine. The aim of the encapsulation is the increase of resistance of the cells to harsh environment or hiding from the host immune system.

*Aspergillus nidulans* is another well-studied fungus that forms long, branching filamentous structures referred to as hyphae. This microorganism is extensively used to produce a wide range of pharmaceutical products. For this purpose *A. nidulans* is grown in bioreactors where it is susceptible to shear forces from agitation and therefore its mechanical properties strongly influence productivity. Zhao *et al* [63] measured by AFM wild type and a mutant strain ( $\Delta\text{csmA}$ ) lacking one of the chitin synthetase genes. Using finite element simulations to fit the data recorded during indentation experiments, the authors deduced Young's modulus of 110 MPa for the wild type and 67 MPa for the mutant.

Readers interested in the exploration of fungal cells by AFM can refer to the following review papers [57, 58, 64, 65].

## 7. Plant cells

Up to now, individual plant cells have only been poorly explored using AFM indentation methods. Pioneering studies

were conducted by Yamada [66] who investigated the elasticity of chloroplasts (and their precursors the etioplasts) of spinach leaves and cucumber seedlings. Chloroplasts are plant cell organelles that, among other chemical reactions, perform photosynthesis. The study revealed that chloroplasts are relatively soft structures (with Young's modulus of 26 kPa) whereas etioplasts are 20 times stiffer. One year later, Clair *et al* [67] used an ultrasonic atomic force microscope [68] to measure the resonance spectra of different wood cell wall layers in order to calculate their mechanical properties. Their measurements revealed, without taking into consideration the inhomogeneity of the sample, values of the cell's Young's modulus ranging between 5 and 20 GPa.

Plant cells are constantly exposed to microorganisms that are potential pathogens, in order to withstand these attacks they have developed various defense mechanisms among which cell wall strengthening plays an important role. These defense mechanisms are not only induced by the presence of pathogen microorganisms but can also be triggered by UV light. Lesniewska *et al* studied by AFM the changes in the cell wall stiffness of grapevine cells upon UV irradiation and measured an increase in stiffness from 72 to 100 MPa [69]. More recently Hayot *et al* [70] studied by AFM the viscoelastic properties of the cell wall of wild type and genetically modified *Arabidopsis thaliana*, probably the most studied plant cell. The authors used finite element methods to model the tip-cell interaction in order to interpret experimental data and to highlight significant differences in the viscoelastic properties between the studied samples. Radotic *et al* [71] used a different technique, stiffness tomography, to explore the static mechanical properties of *A. thaliana* cell wall as a function of time. The study did not

involve the entire plant but only its single cells that were grown in suspension, i.e. dissociated in a liquid medium. The measurements were conducted on living cells at different periods of time during a time-period of three weeks, to follow the evolution of the cell wall stiffness and to highlight modifications in its composition. Stiffness tomography also permitted investigating the distribution of structures inside the cell wall (i.e. at different depths underneath the cell wall surface) as a function of the growth phase.

## 8. Mammalian cells

Since the early 1970s changes in cell mechanical properties have been associated with numerous pathologies such as cancer, cardiovascular affections or diabetes offering the potential to serve as selective disease markers [72]. Moreover, recent results suggest that mechanical forces trigger numerous and important cellular physiological phenomena such as cell morphology, mobility and cellular differentiation [73–75]. This has fuelled the use of AFM-based techniques to characterize the mechanical properties of several living cell types under various physiological and pathological conditions. Erythrocytes from patients suffering from sickle cell disease have been found to be stiffer and more viscous than normal red blood cells [76, 77] and recently Girasole *et al* have highlighted the link between the erythrocyte's ageing, its Young's modulus and its morphological properties [78]. Muscle cells from dystrophin-deficient rat model of Duchenne muscular dystrophy revealed to be much softer than their healthy counterparts [79, 80]. Cancerous cells are particularly intensively explored nowadays since the disease is characterized by major cytoskeleton remodelling and it is well documented that cytoskeletal architecture plays an important role in determining the cell's mechanical properties. Differences in the viscous and elastic properties between normal hepatocytes and hepatocarcinoma cells (liver cancer cells) have been documented by Wu *et al* in 2000 [81]. Cross *et al* [82, 83] reported that metastatic cancer cells are 70% softer than normal cells. These findings with numerous others on other kinds of cancers [84–86] strongly suggest that the nanomechanical analysis could become an efficient cancer diagnostic tool. For instance, recently Plodinec *et al* [87] demonstrated that AFM can efficiently detect breast cancer based on the stiffness of the biopsy specimens.

Due to their specific mechanical characteristics, osteoblasts have been thoroughly investigated using AFM and their nanomechanical properties are now well studied [88, 89] indicating, for instance, that Young's modulus and substrate adhesion of these cells depend considerably on the growth substrate [90], suggesting a direct correlation between these two parameters.

Similarly, fibroblasts are commonly investigated using AFM force analyses to determine, for example, the effects of lesions or infections [91] or the contribution of the substrate [92] to the mechanical and morphological properties of these cells. Recently, by exploiting the higher speed and resolution of the more modern microscopes, Raman *et al* were able to characterize the evolution in time of the mechanical

properties of fibroblasts, as well as of red blood cells and bacteria evidencing, with unprecedented temporal resolution, modifications in the stiffness of the cytoskeleton of these cells [18].

Lymphocytes are among the most important components of the adaptive immune system. Their functions include the recognition of foreign antigens, the activation of other immune cells or the direct activation of various response functions. Since the cell membrane is primarily involved in the immune response, lymphocyte membrane alterations will have a major role in influencing the cell's behaviour. Hu *et al* have compared the ultrastructural and mechanical properties of the membranes in resting, activated and apoptotic lymphocytes demonstrating that the activation causes variations both in morphology and Young's modulus and that this can be associated with modifications in cellular physiology [93].

Due to its high lateral resolution, AFM can target and measure, in living mammalian cells, the stiffness of specific cellular components such as nuclei [94, 95], protein secreting vesicles [96], cytoskeleton components [97] or even cell membrane [98]. By limiting the indentation depth or by considering only a limited segment of the force–distance curve it becomes possible to selectively explore the stiffness of different 'layers' of the cell. This approach permitted Kasas *et al* [97] to discriminate the mechanical contribution of the actin cytoskeleton, located immediately underneath the cell membrane from the contribution of the tubulin, situated deeper underneath the surface. A similar approach permitted the same team to identify and characterize lipid rafts in living neuronal cells [99]. Rafts are specific membrane domains that are enriched in cholesterol and that serve as platforms for numerous receptors, playing an important role in various physiological or pathological processes. The lateral dimensions of the domains are below 200 nm and their thickness less than 10 nm. AFM indentation experiments and a specific data processing technique permitted highlighting that rafts are 30% stiffer than their surrounding membrane.

More recently Roduit *et al* [21, 100] applied stiffness tomography to explore the interior of living nerve cells and macrophages. The resulting 3D stiffness maps revealed a complex and stiff network that is present underneath the cell membrane and that has been demonstrated to correspond to the actin cytoskeleton.

## 9. Conclusions

This review reports only a small portion of the many and high-quality studies that have been aimed at the determination of the nanomechanical properties of biological samples (typically stiffness, Young's modulus, deformability and adhesion). Atomic force microscopy is a powerful technique that permits the exploration of numerous characteristics of biological samples. The high-resolution imaging of cell membranes, the localization and manipulation of individual cell-surface molecules such as receptors and sensors, and the quantification of the sample's mechanical properties offer a powerful means to unravel the fundamental mechanisms of cellular processes. In particular, this latter analysis can

provide valuable information on many areas of cell biology, including physiology, cell membrane structure and dynamics and cytoskeletal dynamics. In fact, local determination of the mechanical properties, combined with high-resolution topography, allows a better understanding of the sample and provides a better insight into the mechanism and function of biosystems. In the near future, improvements in data acquisition and in the speed of recording are expected. This will allow performing fast characterizations of living, evolving systems, opening the way to more complete comparison between local variations in elasticity and morphology.

## Acknowledgment

This work has been supported by FN-CR 32I3-130676 and 200021-144321.

## References

- [1] Binnig G, Quate C F and Gerber C 1986 Atomic force microscope *Phys. Rev. Lett.* **56** 930–3
- [2] Binnig G and Rohrer H 1982 Scanning tunneling microscopy *Helv. Phys. Acta.* **55** 726–35
- [3] Kurland N E, Drira Z and Yadavalli V K 2012 Measurement of nanomechanical properties of biomolecules using atomic force microscopy *Micron* **43** 116–28
- [4] Zhong Q, Inniss D, Kjoller K and Elings V B 1993 Fractured polymer silica fiber surface studied by tapping mode atomic-force microscopy *Surf. Sci.* **290** L688–92
- [5] Weisenhorn A L *et al* 1993 Deformation observed on soft surfaces with an AFM, scanning probe microscopies II *Proc. SPIE Society of Photo-optical Instrumentation Engineers* ed C C Williams **1855** 26–34
- [6] Meyer E *et al* 1988 Comparative-study of lithium-fluoride and graphite by atomic force microscopy (AFM) *J. Microsc.—Oxford* **152** 269–80
- [7] Hertz H 1896 Über die berührung fester elastischer Körper *J. Reine Angew. Math.* **92** 156
- [8] Sneddon I N 1965 The relation between load and penetration in the axisymmetric Boussinesq problem for a punch of arbitrary profile *Int. J. Eng. Sci.* **3** 47–57
- [9] Johnson K L, Kendall K and Roberts A D 1971 Surface energy and contact of elastic solids *Proc. R. Soc. Lond. A* **324** 301–13
- [10] Tataru Y 1989 Extensive theory of force–approach relations of elastic spheres in compression and in impact *J. Eng. Mater. Technol.—Trans. ASME* **111** 163–8
- [11] Cappella B and Dietler G 1999 Force–distance curves by atomic force microscopy *Surf. Sci. Rep.* **34** 1–104
- [12] Butt H J, Cappella B and Kappl M 2005 Force measurements with the atomic force microscope: technique, interpretation and applications *Surf. Sci. Rep.* **59** 1–152
- [13] Ikai A 2008 *The World of Nano-Biomechanics* (Amsterdam: Elsevier)
- [14] Chan Y L and Ngan A H W 2010 Invariant elastic modulus of viscoelastic materials measured by rate-jump tests *Polym. Test.* **29** 558–64
- [15] Zhou Z L, Ngan A H W, Tang B and Wang A X 2012 Reliable measurement of elastic modulus of cells by nanoindentation in an atomic force microscope *J. Mech. Behavior Biomed. Mater.* **8** 134–42
- [16] Martin Y, Williams C C and Wickramasinghe H K 1987 Atomic force microscope force mapping and profiling on a sub 100-Å scale *J. Appl. Phys.* **61** 4723–9
- [17] Tamayo J and Garcia R 1997 Effects of elastic and inelastic interactions on phase contrast images in tapping-mode scanning force microscopy *Appl. Phys. Lett.* **71** 2394–6
- [18] Raman A *et al* 2011 Mapping nanomechanical properties of live cells using multi-harmonic atomic force microscopy *Nature Nanotechnol.* **6** 809–14
- [19] Shekhawat G S and Dravid V P 2005 Nanoscale imaging of buried structures via scanning near-field ultrasound holography *Science* **310** 89–92
- [20] Tetard L *et al* 2008 Imaging nanoparticles in cells by nanomechanical holography *Nature Nanotechnol.* **3** 501–5
- [21] Roduit C, Sekatski S, Dietler G, Catsicas S, Lafont F and Kasas S 2009 Stiffness tomography by atomic force microscopy *Biophys. J.* **97** 674–7
- [22] Singh P, Gonzalez M J and Manchester M 2006 Viruses and their uses in nanotechnology *Drug Dev. Res.* **67** 23–41
- [23] Thundat T *et al* 1992 Calibration of atomic force microscope tips using biomolecules *Scanning Microsc.* **6** 903–10
- [24] Zenhausern F, Adrian M, Emch R, Taborelli M, Jobin M and Descouts P 1992 Scanning force microscopy and cryoelectron microscopy of tobacco mosaic-virus as a test specimen *Ultramicroscopy* **42** 1168–72
- [25] Vesenka J, Manne S, Giberson R, Marsh T and Henderson E 1993 Colloidal gold particles as an incompressible atomic-force microscope imaging standard for assessing the compressibility of biomolecules *Biophys. J.* **65** 992–7
- [26] Falvo M R *et al* 1997 Manipulation of individual viruses: friction and mechanical properties *Biophys. J.* **72** 1396–403
- [27] Ivanovska I L *et al* 2004 Bacteriophage capsids: tough nanoshells with complex elastic properties *Proc. Natl Acad. Sci. USA* **101** 7600–5
- [28] Michel J P *et al* 2006 Nanoindentation studies of full and empty viral capsids and the effects of capsid protein mutations on elasticity and strength *Proc. Natl Acad. Sci. USA* **103** 6184–9
- [29] Carrasco C *et al* 2006 DNA-mediated anisotropic mechanical reinforcement of a virus *Proc. Natl Acad. Sci. USA* **103** 13706–11
- [30] Liashkovich I, Hafezi W, Kuehn J E, Oberleithner H, Kramer A and Shahin V 2008 Exceptional mechanical and structural stability of HSV-1 unveiled with fluid atomic force microscopy *Proc. Natl Acad. Sci. USA* **121** 2287–92
- [31] Roos W H, Radtke K, Kniesmeijer E, Geertsema H, Sodeik B and Wuite G J L 2009 Scaffold expulsion and genome packaging trigger stabilization of herpes simplex virus capsids *Proc. Natl Acad. Sci. USA* **106** 9673–8
- [32] Kol N, Gladnikoff M, Barlam D, Shneck R Z, Rein A and Rouso I 2006 Mechanical properties of murine leukemia virus particles: effect of maturation *Biophys. J.* **91** 767–74
- [33] Kol N *et al* 2007 A stiffness switch in human immunodeficiency virus *Biophys. J.* **92** 1777–83
- [34] Roos W H, Gertsman I, May E R, Brooks C L III, Johnson J E and Wuite G J L 2012 Mechanics of bacteriophage maturation *Proc. Natl Acad. Sci. USA* **109** 2342–7
- [35] Roos W H *et al* 2010 Squeezing protein shells: how continuum elastic models, molecular dynamics simulations, and experiments coalesce at the nanoscale *Biophys. J.* **99** 1175–81
- [36] Arkhipov A, Roos W H, Wuite G J L and Schulten K 2009 Elucidating the mechanism behind irreversible deformation of viral capsids *Biophys. J.* **97** 2061–9
- [37] Baclayon M, Wuite G J L and Roos W H 2010 Imaging and manipulation of single viruses by atomic force microscopy *Soft Matter* **6** 5273–85
- [38] Sears C L 2005 A dynamic partnership: celebrating our gut flora *Anaerobe* **11** 247–51
- [39] Xu W, Mulhern P J, Blackford B L, Jericho M H, Firtel M and Beveridge T J 1996 Modeling and measuring the elastic properties of an archaeal surface, the sheath of

- Methanospirillum hungatei*, and the implication for methane production *J. Bacteriol.* **178** 3106–12
- [40] Amoldi M, Kacher C M, Bauerlein E, Radmacher M and Fritz M 1998 Elastic properties of the cell wall of *Magnetospirillum gryphiswaldense* investigated by atomic force microscopy *Appl. Phys. A* **66** S613–7
- [41] Velegol S B and Logan B E 2002 Contributions of bacterial surface polymers, electrostatics, and cell elasticity to the shape of AFM force curves *Langmuir* **18** 5256–62
- [42] Abu-Lail N I and Camesano T A 2002 Elasticity of *Pseudomonas putida* KT2442 surface polymers probed with single-molecule force microscopy *Langmuir* **18** 4071–81
- [43] Gaboriaud F, Baillet S, Dague E and Jorand F 2005 Surface structure and nanomechanical properties of *Shewanella putrefaciens* bacteria at two pH values (4 and 10) determined by atomic force microscopy *J. Bacteriol.* **187** 3864–8
- [44] Gaboriaud F, Parcha B S, Gee M L, Holden J A and Strugnell R A 2008 Spatially resolved force spectroscopy of bacterial surfaces using force-volume imaging *Colloids Surf. A* **62** 206–13
- [45] Francius G *et al* 2008 Detection, localization, and conformational analysis of single polysaccharide molecules on live bacteria *Acs Nano*. **2** 1921–9
- [46] Pinzón-Arango P A, Nagarajan R and Camesano T A 2010 Effects of L-alanine and inosine germinants on the elasticity of *Bacillus anthracis* spores *Langmuir* **26** 6535–41
- [47] Lau P C Y, Dutcher J R, Beveridge T J and Lam J S 2009 Absolute quantitation of bacterial biofilm adhesion and viscoelasticity by microbead force spectroscopy *Biophys. J.* **96** 2935–48
- [48] Francius G *et al* 2011 Bacterial surface appendages strongly impact nanomechanical and electrokinetic properties of *Escherichia coli* cells subjected to osmotic stress *PLoS One* **6** e20066
- [49] Arce F T *et al* 2009 Nanoscale structural and mechanical properties of nontypeable *Haemophilus influenzae* biofilms *J. Bacteriol.* **191** 2512–20
- [50] Arnal L *et al* 2012 Adhesion contribution to nanomechanical properties of the virulent *Bordetella pertussis* envelope *Langmuir* **28** 7461–9
- [51] Longo G *et al* 2012 Force volume and stiffness tomography investigation on the dynamics of stiff material under bacterial membranes *J. Mol. Recognit.* **25** 278–84
- [52] Dorobantu L S and Gray M R 2010 Application of atomic force microscopy in bacterial research *Scanning* **32** 74–96
- [53] Dupres V, Alsteens D, Andre G and Dufrêne Y F 2010 Microbial nanoscopy: a closer look at microbial cell surfaces *Trends Microbiol.* **18** 397–405
- [54] Scheuring S and Dufrêne Y F 2010 Atomic force microscopy: probing the spatial organization, interactions and elasticity of microbial cell envelopes at molecular resolution *Mol. Microbiol.* **75** 1327–36
- [55] Wright C J, Shah M K and Powell L C 2010 Armstrong: I. Application of AFM from microbial cell to biofilm *Scanning* **32** 134–49
- [56] Dufrêne Y F 2001 Application of atomic force microscopy to microbial surfaces: from reconstituted cell surface layers to living cells *Micron* **32** 153–65
- [57] Dufrêne Y F 2002 Atomic force microscopy, a powerful tool in microbiology *J. Bacteriol.* **184** 5205–13
- [58] Wright C J and Armstrong I 2006 The application of atomic force microscopy force measurements to the characterisation of microbial surfaces *Surf. Interface Anal.* **38** 1419–28
- [59] Arfsten J, Leupold S, Bradtmoeller C, Kampen I and Kwade A 2010 Atomic force microscopy studies on the nanomechanical properties of *Saccharomyces cerevisiae* *Colloids Surf. B* **79** 284–90
- [60] Touhami A, Nysten B and Dufrêne Y F 2003 Nanoscale mapping of the elasticity of microbial cells by atomic force microscopy *Langmuir* **19** 4539–43
- [61] Lipke P N and Ovalle R 1998 Cell wall architecture in yeast: new structure and new challenges *J. Bacteriol.* **180** 3735–40
- [62] Svaldo-Lanero T *et al* 2007 Morphology, mechanical properties and viability of encapsulated cells *Ultramicroscopy* **107** 913–21
- [63] Zhao L M, Schaefer D, Xu H X, Modi S J, LaCourse W R and Marten M R 2005 Elastic properties of the cell wall of *Aspergillus nidulans* studied with atomic force microscopy *Biotechnol. Prog.* **21** 292–9
- [64] Dufrêne Y F 2010 Atomic force microscopy of fungal cell walls: an update *Yeast* **27** 465–71
- [65] Gaboriaud F and Dufrêne Y F 2007 Atomic force microscopy of microbial cells: application to nanomechanical properties, surface forces and molecular recognition forces *Colloids Surf. B-Biointerfaces* **54** 10–19
- [66] Yamada T, Arakawa H, Okajima T, Shimada T and Ikai A 2002 Use of AFM for imaging and measurement of the mechanical properties of light-convertible organelles in plants *Ultramicroscopy* **91** 261–8
- [67] Clair B, Arinero R, Leveque G, Ramonda M and Thibaut B 2003 Imaging the mechanical properties of wood cell wall layers by atomic force modulation microscopy *Iawa J.* **24** 223–30
- [68] Yamanaka K and Nakano S 1996 Ultrasonic atomic force microscope with overtone excitation of cantilever *Japan. J. Appl. Phys. Part 1* **35** 3787–92
- [69] Lesniewska E, Adrian M, Klinguer A and Pugin A 2004 Cell wall modification in grapevine cells in response to UV stress investigated by atomic force microscopy *Ultramicroscopy* **100** 171–8
- [70] Hayot C M, Forouzesh E, Goel A, Avramova Z and Turner J A 2012 Viscoelastic properties of cell walls of single living plant cells determined by dynamic nanoindentation *J. Exp. Botany* **63** 2525–40
- [71] Radotic K *et al* 2012 Atomic force microscopy stiffness tomography on living *Arabidopsis thaliana* cells reveals the mechanical properties of surface and deep cell-wall layers during growth *Biophys. J.* **103** 386–94
- [72] Costa K D 2003 Single-cell elastography: probing for disease with the atomic force microscope *Disease Markers* **19** 139–54
- [73] Janmey P A, Winer J P, Murray M E and Wen Q 2009 The hard life of soft cells *Cell Motility Cytoskeleton* **66** 597–605
- [74] Zaman M H *et al* 2006 Migration of tumor cells in 3D matrices is governed by matrix stiffness along with cell-matrix adhesion and proteolysis *Proc. Natl Acad. Sci. USA* **103** 10889–94
- [75] Engler A J, Griffin M A, Sen S, Bonnetnann C G, Sweeney H L and Discher D E 2004 Myotubes differentiate optimally on substrates with tissue-like stiffness: pathological implications for soft or stiff microenvironments *J. Cell Biol.* **166** 877–87
- [76] Brandao M M *et al* 2003 Optical tweezers for measuring red blood cell elasticity: application to the study of drug response in sickle cell disease *Eur. J. Haematol.* **70** 207–11
- [77] Nash G B, Johnson C S and Meiselman H J 1984 Mechanical-properties of oxygenated red-blood-cells in sickle-cell (HBSS) disease *Blood* **63** 73–82
- [78] Girasole M *et al* 2010 The how, when, and why of the aging signals appearing on the human erythrocyte membrane: an atomic force microscopy study of surface roughness *Nanomed.—Nanotechnol. Biol. Med.* **6** 760–8
- [79] Pasternak C, Wong S and Elson E L 1995 Mechanical function of dystrophin in muscle-cells *J. Cell Biol.* **128** 355–61

- [80] Puttini S *et al* 2009 Gene-mediated restoration of normal myofiber elasticity in dystrophic muscles *Mol. Ther.* **17** 19–25
- [81] Wu Z Z, Zhang G, Long M, Wang H B, Song G B and Cai S X 2000 Comparison of the viscoelastic properties of normal hepatocytes and hepatocellular carcinoma cells under cytoskeletal perturbation *Biorheology* **37** 279–90
- [82] Cross S E, Jin Y-S, Rao J and Gimzewski J K 2007 Nanomechanical analysis of cells from cancer patients *Nature Nanotechnol.* **2** 780–3
- [83] Cross S E, Jin Y-S, Tondre J, Wong R, Rao J and Gimzewski J K 2008 AFM-based analysis of human metastatic cancer cells *Nanotechnology* **19** 384003
- [84] Li Q S, Lee G Y H, Ong C N and Lim C T 2008 AFM indentation study of breast cancer cells *Biochem. Biophys. Res. Commun.* **374** 609–13
- [85] Lekka M, Laidler P, Gil D, Lekki J, Stachura Z and Hryniewicz A Z 1999 Elasticity of normal and cancerous human bladder cells studied by scanning force microscopy *Eur. Biophys. J. Biophys. Lett.* **28** 312–6
- [86] Lekka M *et al* 2012 Cancer cell detection in tissue sections using AFM *Arch. Biochem. Biophys.* **518** 151–6
- [87] Plodinec M *et al* 2012 The nanomechanical signature of breast cancer *Nature Nanotechnol.* **7** 757–65
- [88] Soumetz F C, Saenz J F, Pastorino L, Ruggiero C, Nosi D and Raiteri R 2010 Investigation of integrin expression on the surface of osteoblast-like cells by atomic force microscopy *Ultramicroscopy* **110** 330–8
- [89] Simon A *et al* 2003 Characterization of dynamic cellular adhesion of osteoblasts using atomic force microscopy *Cytometry A* **54** 36–47
- [90] Domke J, Dannohl S, Parak W J, Muller O, Aicher W K and Radmacher M 2000 Substrate dependent differences in morphology and elasticity of living osteoblasts investigated by atomic force microscopy *Colloids Surf. B* **19** 367–79
- [91] Reich A, Meurer M, Eckes B, Friedrichs J and Muller D J 2009 Surface morphology and mechanical properties of fibroblasts from scleroderma patients *J. Cell Mol. Med.* **13** 1644–52
- [92] Solon J, Levental I, Sengupta K, Georges P C and Janmey P A 2007 Fibroblast adaptation and stiffness matching to soft elastic substrates *Biophys. J.* **93** 4453–61
- [93] Hu M, Wang J, Zhao H, Dong S and Cai J 2009 Nanostructure and nanomechanics analysis of lymphocyte using AFM: from resting, activated to apoptosis *J. Biomech.* **42** 1513–9
- [94] Guilak F, Tedrow J R and Burgkart R 2000 Viscoelastic properties of the cell nucleus *Biochem. Biophys. Res. Commun.* **269** 781–6
- [95] Broers J L V *et al* 2004 Decreased mechanical stiffness in LMNA-/- cells is caused by defective nucleo-cytoskeletal integrity: implications for the development of laminopathies *Human Mol. Gen.* **13** 2567–80
- [96] A-Hassan E *et al* 1998 Relative microelastic mapping of living cells by atomic force microscopy *Biophys. J.* **74** 1564–78
- [97] Kasas S *et al* 2005 Superficial and deep changes of cellular mechanical properties following cytoskeleton disassembly *Cell Motility Cytoskeleton* **62** 124–32
- [98] Roduit C *et al* 2008 Elastic membrane heterogeneity of living cells revealed by stiff nanoscale membrane domains *Biophys. J.* **94** 1521–32
- [99] Yersin A *et al* 2007 Elastic properties of the cell surface and trafficking of single AMPA receptors in living hippocampal neurons *Biophys. J.* **92** 4482–9
- [100] Roduit C *et al* 2012 Stiffness tomography exploration of living and fixed macrophages *J. Mol. Recognit.* **25** 241–6